JACS
JOURNAL OF THE AMERICAN CHEMICAL SOCIETY

Editors' Choice
Open Access

pubs.acs.org/JACS

Article

Repurposing a Catalytic Cycle for Transient Self-Assembly

Shuntaro Amano* and Thomas M. Hermans*

Cite This: J. Am. Chem. Soc. 2024, 146, 23289−23296

Read Online

ACCESS | Metrics & More | Article Recommendations | Supporting Information

ABSTRACT: Life operates out of equilibrium to enable various sophisticated behaviors. Synthetic chemists have strived to mimic biological nonequilibrium systems in such fields as autonomous molecular machines and dissipative self-assembly. Central to these efforts has been the development of new chemical reaction cycles, which drive systems out of equilibrium by conversion of chemical fuel into waste species. However, the construction of reaction cycles has been challenging due to the difficulty of finding compatible reactions that constitute a cycle. Here, we realize an alternative approach by repurposing a known catalytic cycle as a chemical reaction cycle for driving dissipative self-assembly. This approach can overcome the compatibility problem because all steps involved in a catalytic cycle are already known to proceed concurrently under the same conditions. Our repurposing approach is applicable to diverse combinations of catalytic cycles and systems to drive out of equilibrium, which will substantially broaden the scope of out-of-equilibrium systems.

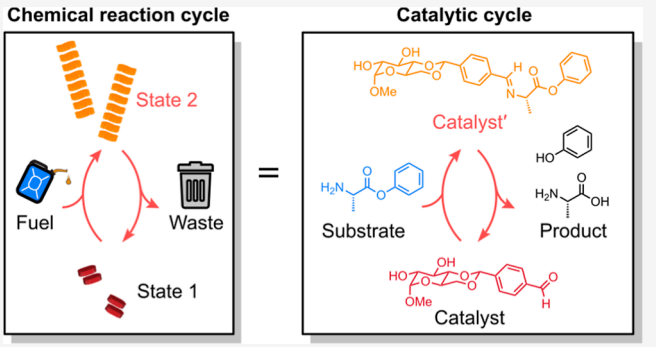

INTRODUCTION

Biological systems operate out of equilibrium to enable various functions that are indispensable to sustain a living state, such as transportation and motility,[1,2] temporal control,[3] and information processing.[4] Inspired by biology, synthetic chemists have sought to develop out-of-equilibrium systems in such areas as molecular machines,[5−7] dissipative self-assembly,[8,9] active materials,[10] and feedback-controlled systems,[11,12] leading to the emergence of the field of systems chemistry.[13−15] In order to drive systems out of equilibrium, energy needs to be supplied.[16] One of the most widely used energy sources is chemical energy; in biology mostly ATP and GTP.[2,17,18] The central element in a system for harnessing chemical energy is a reaction cycle,[19−23] in which chemical fuel[24] is converted into waste species, and the species mediating this conversion travels between different states ("state 1" and "state 2" in Figure 1A). A common approach for constructing new chemical reaction cycles is to combine multiple reactions (Figure 1A, top). The individual reactions can be either catalytic[25−35] or noncatalytic[36−44] and can incorporate enzymatic reactions.[45−50] With biomolecules such as nucleic acids and enzymes, high specificity can be achieved, and multiple reactions proceed concurrently under the same conditions. However, constructing chemical reaction cycles out of small synthetic molecules and coupling them to other driven processes [e.g., (co)conformational changes for molecular machines, self-assembly for dissipative self-assembly] has been challenging. Specifically, it is difficult to find compatible reactions that proceed under the same conditions for constructing a cycle. Even if feasible combinations are found, the resulting reaction cycles often suffer from problems such as fast background fuel decomposition and formation of side products.[19,22]

Here, we realize a simple and general way to design new chemical reaction cycles, which is to repurpose a known catalytic cycle. In contrast to previous reaction cycles that combine multiple reactions and therefore often experience unwanted cross-reactivity, our current approach uses inherently compatible reactions since they have been taken from a known catalytic cycle. Note the equivalence of a chemical reaction cycle and a catalytic reaction cycle (Figure 1A, bottom). Normally, a catalytic reaction is viewed as the conversion of a substrate into a product. However, it can also be viewed as cycling of the catalytic species via two or more states with net directionality, which is equivalent to a chemical reaction cycle. From this perspective, the substrate and the product of a catalytic cycle can be regarded as fuel and waste of a chemical reaction cycle, respectively.

In this study, we combine an aldehyde species (**1** in Figure 1B)[43,51] that catalyzes ester hydrolysis,[52−54] thereby accumulating a transient intermediate (imine ester **4**) that self-assembles into aster-like structures. The amount of the transient intermediate can be tuned by varying the pH, and the cycle can be refueled under specific (pH) conditions.

Received: April 29, 2024
Revised: July 10, 2024
Accepted: July 11, 2024
Published: August 11, 2024

https://doi.org/10.1021/jacs.4c05871
J. Am. Chem. Soc. 2024, 146, 23289−23296

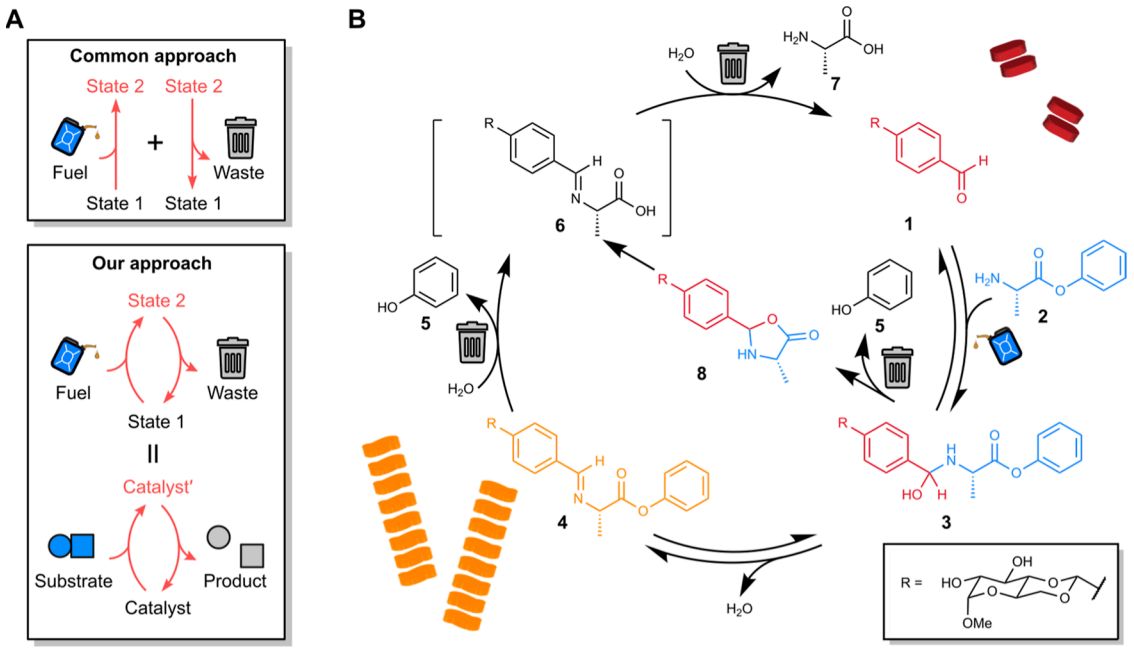

Figure 1. Repurposing an aldehyde-catalyzed ester hydrolysis reaction to induce transient self-assembly. (A) Top: common approach for constructing a chemical reaction cycle, which is to find multiple reactions that proceed under the same conditions and combine them. Bottom: our approach of repurposing a catalytic cycle as a chemical reaction cycle, which is based on the equivalence of these two cycles. A fuel molecule (substrate) reacts with a system's component in state 1 (catalyst), converting it into another state (state 2/catalyst'). The new state undergoes another transformation and returns to the initial state while releasing a waste molecule (product). (B) Reaction cycle of an aldehyde-catalyzed ester hydrolysis. Free catalyst aldehyde **1** and imine ester **4** have different propensity to self-assemble. While chemical fuel **2** is present, the assembly of imine ester **4** is formed transiently. Dimerization of ester fuel **2** also occurs but is omitted for clarity.

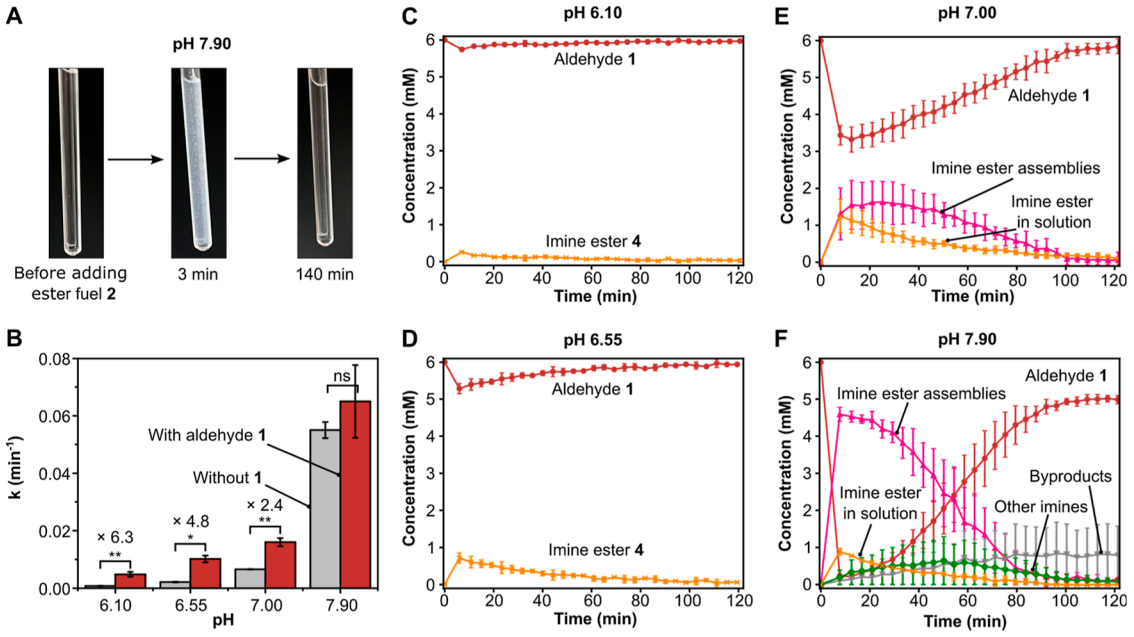

Figure 2. Fuel addition experiments to aldehyde **1** solution. (A) Reaction mixture at pH = 7.90 before adding ester fuel **2** and 3 and 140 min after the fuel addition. Transient formation of visible assemblies of imine ester **4** was observed. (B) Observed pseudo-first-order rate constants for fuel consumption with and without aldehyde **1** (k_{cat} and k_{uncat}, respectively) at different pH values. The numbers on each set of bar graphs are the magnitude of acceleration, k_{cat}/k_{uncat}. Error bars represent standard errors obtained from duplicate experiments. ns = (not significant), * and ** mean that the *P* value of statistical testing is ≥0.05, 0.01 to 0.05, and 0.001 to 0.01, respectively. See Section S7 for details. (C–F) Concentration changes of catalyst-containing species over time. Error bars represent standard errors obtained from duplicate experiments (panel C,D) or four replicates (panel E,F). "Imine ester assemblies" signify the visible aster-like assemblies of imine ester **4**. Reaction conditions: aldehyde **1** (6 mM); ester fuel **2** (48 mM, 8 equiv); MES or HEPES buffer (200 mM) at pH = 6.10, 6.55, 7.00 or 7.90; D_2O; and 293 K.

Catalysis has been broadly studied in the context of reaction development, where the main goal is to optimize catalytic reactions for production by improving the conversion rate, turnover number, and selectivity. Nevertheless, little attention

https://doi.org/10.1021/jacs.4c05871
J. Am. Chem. Soc. 2024, 146, 23289−23296

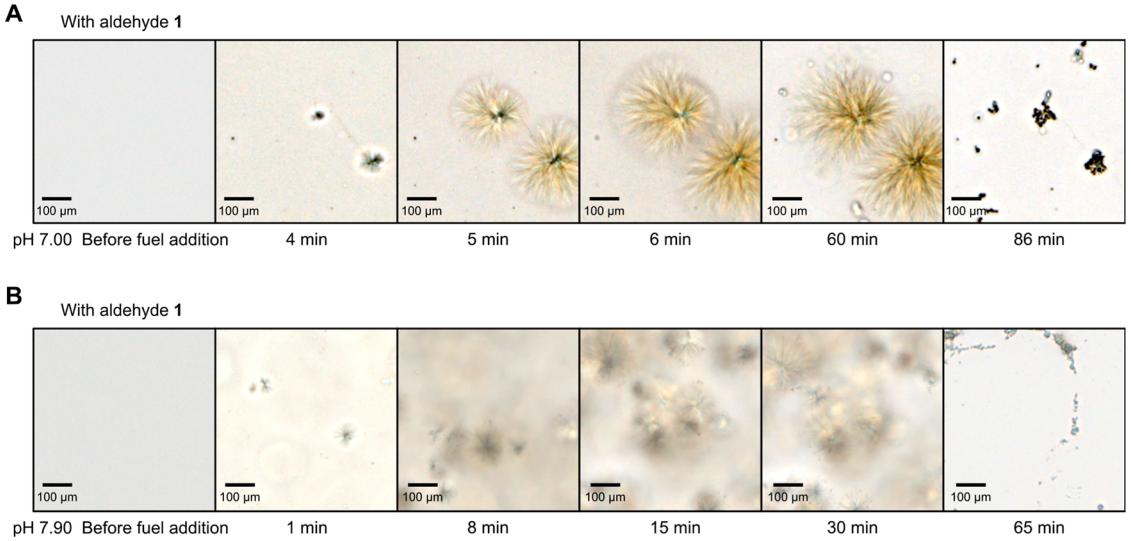

Figure 3. Optical microscopy images of imine ester assemblies **4** at designated time points at (A) pH = 7.00 and (B) 7.90. Emergence and disappearance of aster-like structures could be observed. The assembly size at pH = 7.90 was smaller than at pH = 7.00, due to faster formation of imine ester **4** and more frequent nucleation events. The last images at each pH show trace amount of deposits formed on the cover glass during the reaction. Reaction conditions: aldehyde **1** (6 mM), ester fuel **2** (48 mM, 8 equiv), MES or HEPES buffer (200 mM), D_2O, and room temperature.

has been paid to the accumulation of intermediate species in the catalytic cycle, which is our target. The recognition that catalytic cycles are indeed chemical reaction cycles suggests that already well-studied catalytic cycles may be reused as useful elements for constructing synthetic out-of-equilibrium systems. The approach of repurposing known catalytic cycles is versatile and applicable to diverse combinations of catalytic cycles (e.g., organocatalysts,[55] organometallic catalysts[56]) and systems to drive out of equilibrium (e.g., dissipative self-assembly,[8,9] molecular machines[5−7]), substantially enriching the toolbox of synthetic out-of-equilibrium systems.

RESULTS AND DISCUSSION

Reaction Cycle of Ester Fuel Hydrolysis Catalyzed by an Aldehyde Species. In this study, we combined an aldehyde species **1** and a reported reaction catalyzed by aromatic aldehydes, namely a hydrolysis of amine esters such as **2** (Figure 1B).[52] According to the literature and our analysis of the reaction progress (see the next section), the reaction cycle consists of two pathways. In both pathways, aldehyde **1** first reacts with ester fuel **2** to generate hemiaminal **3**. In the first pathway, this intermediate undergoes water elimination to generate imine ester **4**, which is hydrolyzed stepwise to regenerate aldehyde **1**. In the second pathway, hemiaminal **3** is transformed to lactone **8** via intramolecular cyclization, which undergoes ring-opening and hydrolysis to regenerate aldehyde **1**. Overall, this reaction cycle hydrolyzes ester fuel **2** into two waste species, phenol **5** and alanine **7**. It is the first pathway that enabled accumulation of transient imine ester **4** that forms macroscopic aster-like structures.

Transient Formation of Imine Ester Assemblies in the Aldehyde-Catalyzed Fuel Consumption Reaction. We conducted fueling experiments by adding ester fuel **2** to a solution of aldehyde **1** in buffer at pH = 6.10, 6.55, 7.00, and 7.90. At pH = 7.00 and 7.90, we observed formation of white insoluble species, which gradually disappeared over time (Figure 2A, see Figure S5C for images at pH = 7.00). These species were characterized to be imine ester **4** by ^{1}H NMR and mass spectrometry (Section S4.3, see Section S4.4 for characterization of **4** in solution). Aldehyde **1** is known to self-assemble in aqueous conditions,[43,51] but imine ester **4** has higher propensity to self-assemble because of its increased hydrophobicity. Consequently, in the reported experimental conditions, aldehyde **1** did not form any visible structures, whereas imine ester **4** formed visible aster-like structures. For understanding the system's behavior in more detail, we tracked the concentration change of each species by ^{1}H NMR. The concentration profiles of ester fuel **2** were fitted to a pseudo-first-order kinetic model for quantifying the rate of fuel decomposition (Figures S4B and S5B). The comparison of rate constants for experiments with and without aldehyde **1** (k_{cat} and k_{uncat}, respectively) at the same pH confirmed that the catalytic effect by aldehyde **1** was present at pH = 6.10, 6.55, and 7.00 (Figure 2B). As the pH increased, the magnitude of acceleration (k_{cat}/k_{uncat}) decreased from 6.3 to 2.4, whereas the absolute rate of fuel decomposition increased concurrently. The concentration profiles of catalyst-containing species were also obtained (Figure 2C−F). The maximum concentration of imine ester **4** constantly increased as the pH was increased. Beyond a certain concentration, the formation of visible assemblies of imine ester **4** could be observed (pH = 7.00 and 7.90). The conversion to imine ester **4** reached 93% (pH = 7.90). Both imine ester **4** in solution and visible imine ester assemblies gradually decomposed as ester fuel **2** ran out.

The emergence and disappearance of assemblies of imine ester **4** were observed by optical microscopy techniques (Figure 3, Section S4.5 and Videos S1 and S2). At both pH = 7.00 and 7.90, the assemblies had globular aster-like structures. The size of each assembly was smaller at pH = 7.90 than at pH = 7.00. This is probably due to the different rates of imine ester formation: the generation of imine ester **4** was faster at pH = 7.90 and nucleation occurred more frequently. As a result, the imine ester assemblies at pH = 7.90 became larger in number but smaller in size than those at pH = 7.00. Interestingly, at pH = 7.00 the reaction cycle could be repeated 3 times without damping (see Figure S8a−c).

Investigation of the System's Mechanism. In order to investigate further the mechanism behind the transient

https://doi.org/10.1021/jacs.4c05871
J. Am. Chem. Soc. 2024, 146, 23289−23296

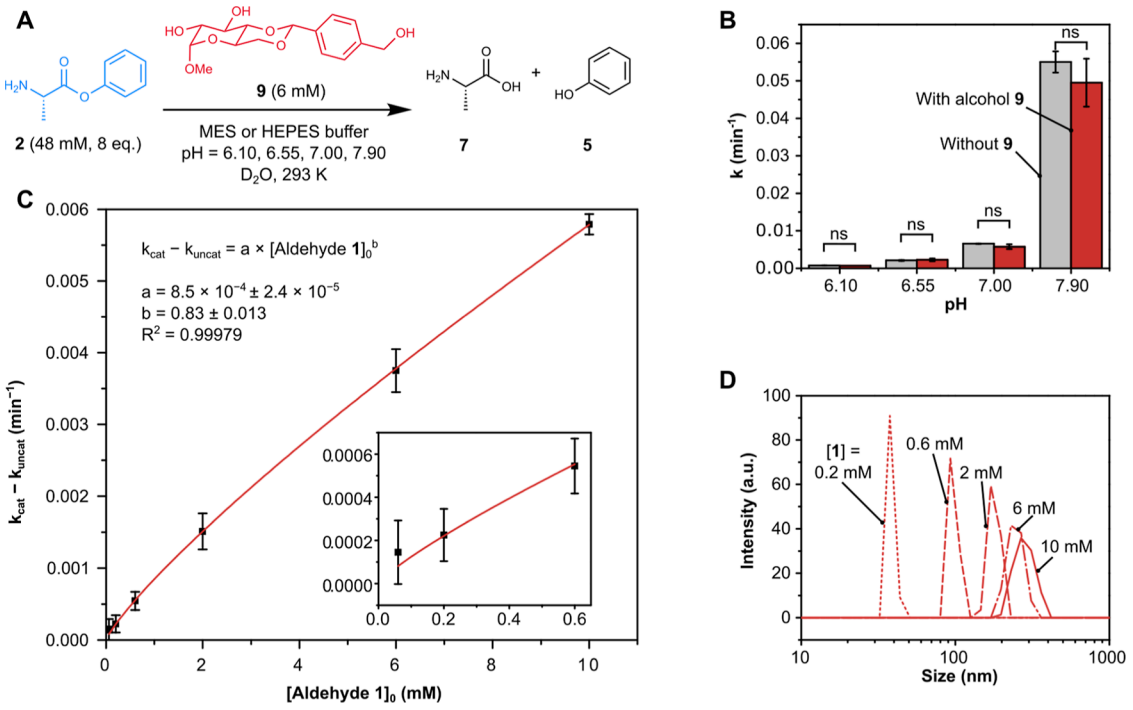

Figure 4. Investigation of the reaction mechanism of ester fuel hydrolysis catalyzed by aldehyde **1**. (A) Reaction scheme of ester fuel hydrolysis experiments in the presence of alcohol **9**, which has a similar structure to aldehyde **1** but lacks a formyl group. (B) Observed pseudo-first-order rate constants for fuel consumption with and without alcohol **9** (k_{cat} and k_{uncat}, respectively) at different pH values. Error bars represent standard errors obtained from duplicate experiments. ns (not significant) means that the *P* value of statistical testing is ≥0.05. See Section S7 for details. (C) Rate of catalyzed processes at different concentrations of aldehyde catalyst **1**. Reaction conditions: aldehyde **1** (0.06, 0.2, 0.6, 2, 6, or 10 mM), ester fuel **2** (48 mM), MES buffer (200 mM) at pH = 6.10, D_2O, and 293 K. The black markers depict the rates of catalyzed processes measured in the ^{1}H NMR experiments, with the error bars that show standard errors obtained from duplicate experiments. The red line is the result of nonlinear fitting to the equation at the top-left corner, where "*a*" and "*b*" are the fitted parameters. The inset is a magnification of the low-concentration region. (D) DLS measurements of aldehyde **1** (0.2, 0.6, 2, 6, and 10 mM) solution at pH = 6.10. The DLS measurement of aldehyde **1** solution at 0.06 mM did not yield any reliable signal.

accumulation of imine ester **4**, we conducted a set of control experiments. First, operation experiments were attempted with alcohol **9** as a catalyst, which has a structure similar to that of aldehyde **1** but lacks a formyl group (Figure 4A). These experiments did not show any acceleration in the fuel decomposition. The pseudo-first-order rate constants of the decomposition with and without alcohol **9** did not show statistically significant difference at all pH values (Figure 4B). This corroborates the reaction mechanism of catalysis depicted in Figure 1B, which requires a formyl group as a crucial element. We also discovered that alcohol **9** forms self-assembled structures of the size comparable to aldehyde **1** (Figure S15D). Therefore, the catalysis by **1** is not likely to be caused by functional groups other than the formyl group that are in close proximity in the self-assemblies of aldehyde **1**.

Next, catalytic fuel hydrolysis with different concentrations of aldehyde **1** was attempted. We fixed the pH at 6.10 for this study because this pH showed the largest rate acceleration by catalysis among the pH values employed in the study (Figure 2B). This allowed us to study the effect of the catalyst concentration to the fuel decomposition rate more accurately by having a large variation in the reaction rate. By subtracting the rate constants in absence of aldehyde **1** (k_{uncat}) from the rate constants in the presence of **1** (k_{cat}), the rate constants for the catalytic fuel hydrolysis (i.e., processes that involve aldehyde **1**) were calculated ($k_{cat} - k_{uncat}$, see Section S5.2 for detailed discussion). The catalysis rate increased almost linearly as the initial concentration of aldehyde **1** (shown as $[\mathbf{1}]_0$) increased (Figure 4C). Nonlinear fitting showed that the exponent to $[\mathbf{1}]_0$ ("*b*" in the top-left equation in Figure 4C) was 0.83 ± 0.013. This value becomes one in the case of genuinely linear dependence, and the obtained value, 0.83 ± 0.013, is close to one. To probe the nature of the catalytically active species, we further studied the assembly state of aldehyde **1** at different concentrations. Dynamic light scattering (DLS) measurements demonstrated the presence of large assembled structures of aldehyde **1** even at $[\mathbf{1}]_0$ = 0.2 mM (Figure 4D). This suggests that the increase of $[\mathbf{1}]_0$ beyond 0.2 mM led to the formation of more of assembled structures, while keeping the concentration of monomeric aldehyde nearly constant, because the self-assembly mechanism of this aldehyde is cooperative:[57] in the cooperative formation of supramolecular polymer, the concentration of a nonassembling monomer remains constant once the total monomer concentration exceeds the critical aggregation concentration.[58,59] Therefore, the increase in the catalysis rate at higher $[\mathbf{1}]_0$ is most likely the consequence of the increase in the amount of assembled structures, and we conclude that the catalysis of the fuel hydrolysis involves not only monomeric aldehyde **1** but also their assemblies. Still, the exponent to $[\mathbf{1}]_0$ in the nonlinear fitting (b = 0.83 ± 0.013 in Figure 4C) is smaller than one. We ascribe this discrepancy to the shielding effect in the assembled structures:[59] the larger the assemblies become, the more shielded the inner monomers are from the solution phase, preventing them to participate in catalysis.

Kinetic Modeling Based on Experiments with a Model Aldehyde. In order to study the effect of changing the rate of

https://doi.org/10.1021/jacs.4c05871
J. Am. Chem. Soc. 2024, 146, 23289−23296

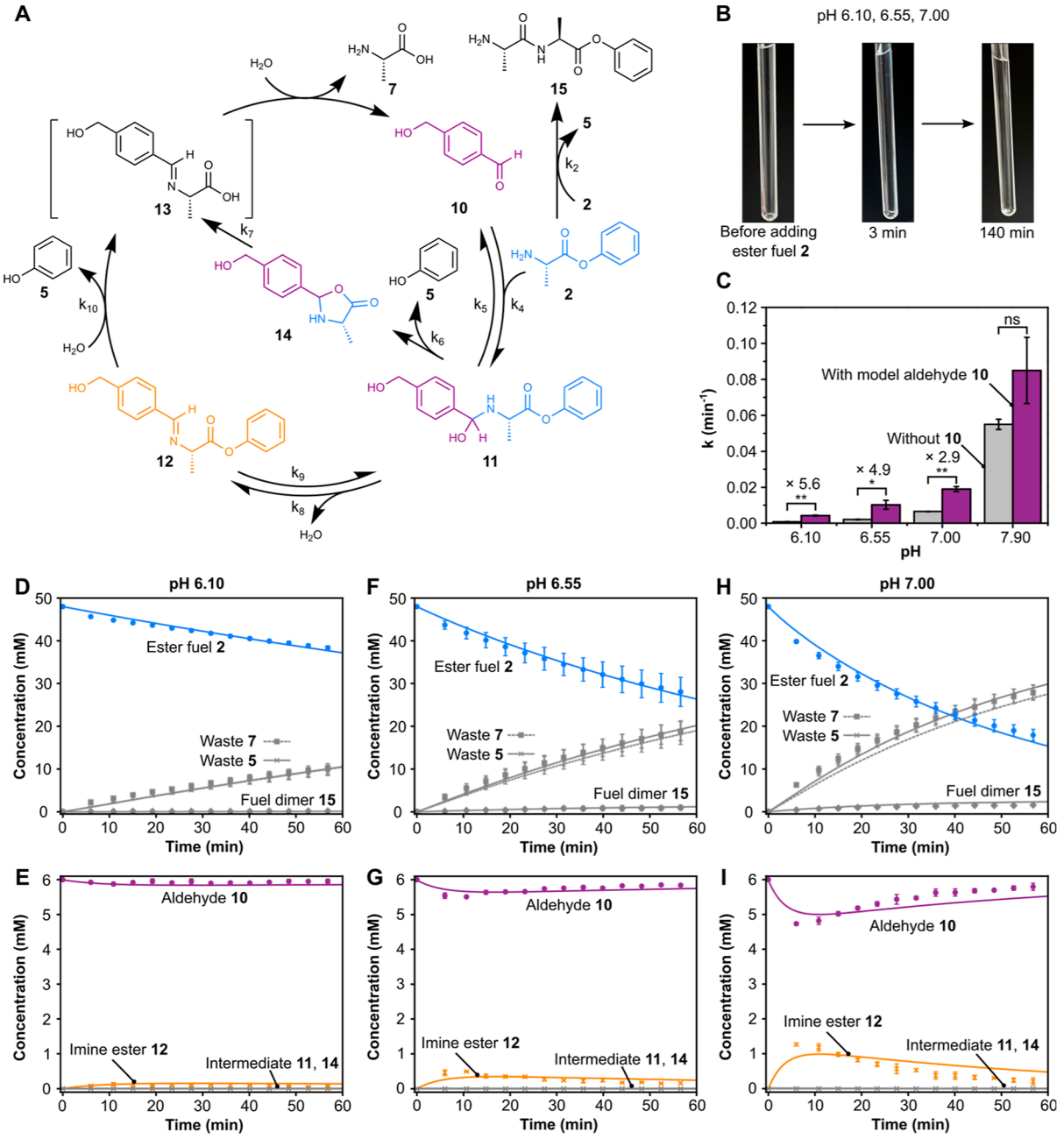

Figure 5. Construction of a kinetic model based on experiments with model aldehyde **10**. (A) Reaction cycle of ester fuel hydrolysis catalyzed by model aldehyde **10**. k_2 and k_4–k_{10} are rate constants for reactions. k_1 and k_3 are the rate constants for the background fuel hydrolysis reaction and the hydrolysis of fuel dimer **15**, respectively. They are omitted for clarity in the figure. (B) Reaction mixture with model aldehyde **10** at pH = 7.00 before adding ester fuel **2**, at 3 and 140 min after the fuel addition. No visible assemblies were observed. Similar results were observed at pH = 6.10 and pH = 6.55, whereas transient formation of visible assemblies was observed at pH = 7.90. (C) Observed pseudo-first-order rate constants for fuel consumption with and without model aldehyde **10** (k_{cat} and k_{uncat}, respectively) at different pH values. The numbers on each set of bar graphs are the magnitude of acceleration, k_{cat}/k_{uncat}. Error bars represent standard errors obtained from duplicate experiments. ns (not significant), * and ** mean that the *P* value of statistical testing is ≥0.05, 0.01 to 0.05, and 0.001 to 0.01, respectively. See Section S7 for details. (D–I) Concentration changes of fuel **2**, waste **5**, waste **7**, and fuel dimer **15** species (D,F,H) and catalyst-containing species (E,G,I) over time at different pH values. Note that the reactions were monitored for 60 min, not 120 min. Scatter: experimental results and line: fitted model. Error bars represent standard errors obtained from duplicate experiments. Reaction conditions: model aldehyde **10** (6 mM); ester fuel **2** (48 mM, 8 equiv); MES or HEPES buffer (200 mM) at pH = 6.10, 6.55, 7.00 or 7.90; D_2O; and 293 K.

each step in the system and understand how the change in pH affects the amount of accumulated imine ester **4**, we developed a kinetic model. The model is based on experiments with model aldehyde **10**, as well as on previous studies[52,60,61] (Figure 5A). We used this model aldehyde since it has a lower propensity to self-assemble than aldehyde **1**. Upon fuel addition, it did not form visible assembled structures not only at pH = 6.10 and 6.55 but also at pH = 7.00 (Figures 5B and S17C), while aldehyde **1** formed visible assemblies at pH = 7.00 (Figure S5C. See Figure S17D for DLS measurements of model aldehyde **10** solutions). This property of model aldehyde **10** enabled us to develop a rather simple kinetic model that does not need to consider large

https://doi.org/10.1021/jacs.4c05871
J. Am. Chem. Soc. 2024, 146, 23289–23296

self-assembled structures that crush out from solution. The catalytic reaction cycle of this system resembles the one with original aldehyde **1** (Figure 5A, see Section S6.2 for the full description of the kinetic model). Also, the magnitudes of acceleration of the fuel decomposition with model aldehyde **10** were similar to those of aldehyde **1** at all pH values (Figure 5C, see Section S7 for statistical comparison of the fuel decomposition rates with aldehyde **1** and model aldehyde **10**), which justifies the use of **10** as a model compound. The fitted model agreed well with experimentally observed concentrations of the fuel and waste species and could reproduce transient accumulation of imine ester **12** (Figure 5D−I). The fitting of the kinetic model was attempted only for the experiment results at pH = 6.10, 6.55, and 7.00 because visible assemblies were observed at pH = 7.90 (see Figure S17E,F for the experiment result at pH = 7.90).

Based on these fitting results, we systematically varied the rate constants concerning the catalytic cycle (k_4−k_{10}) and examined their effects (Section S6.3). Depending on the rate constant to vary, three types of effects were observed at all pH values. When k_4 or k_8 was increased, or k_5 or k_9 was decreased, the consumption of ester fuel **2** was accelerated and more transient imine ester **12** was formed. This effect originates from the shift of the imine-formation equilibria to the product side, resulting in the accumulation of hemiaminal **11** or imine ester **12**. When k_6 or k_{10} was increased, the consumption of ester fuel **2** was accelerated while less transient imine ester **12** formed. This is because the faster consumption of hemiaminal **11** or imine ester **12** decreased the amount of accumulated imine ester. Finally, the variation in k_7 had no observable effect as long as $k_7 \gg k_6$, which is an experimentally validated condition.[52] The variation in pH has different effects on each of these three types of the reactions. Previous studies suggest that k_6 and k_{10} are larger at a higher pH.[52] As was examined before, these rate accelerations should decrease the amount of transient imine ester **12**. However, our experimental observations showed the opposite trend: the higher the pH, the more imine ester **12** formed. Considering the neutrality of k_7 to the system's behavior, it is likely that the change in k_4, k_5, k_8, and/or k_9, which shifts the imine-formation equilibria, increased the imine ester accumulation at a higher pH. Indeed, a study of imine formation in aqueous solution demonstrated that imine-formation equilibria shift to the imine side at a higher pH (see Section S6.3 for a more detailed discussion).[60] Our results demonstrate that the accumulation of transient species can be tuned by varying reaction conditions (e.g., pH), which has a broader implication to our repurposing approach: even if such accumulation is not reported in the original literature of a catalytic reaction, we may still be able to utilize its catalytic cycle as a reaction cycle to accumulate transient species (and for causing other nonequilibrium behaviors) by varying the reaction conditions.

CONCLUSIONS

In this study, we repurposed a known catalytic cycle as a chemical reaction cycle to induce a nonequilibrium behavior and could accumulate self-assembling species transiently. Moreover, the amount of the transient species could be tuned by varying a reaction condition (pH), and the cycle could be refueled multiple times (at pH = 7.00). Our approach is simple and general and potentially applicable to diverse combinations of catalytic cycles and systems to drive out of equilibrium. For example, organocatalytic cycles may prove facile elements for constructing out-of-equilibrium systems due to their mechanistic simplicity and easy handling.[55] More conventional catalytic cycles of organometallic[56] and heterogeneous[62] catalysis may also be useful for this purpose due to their diversity in the catalyzed reactions. These catalytic cycles can be combined to a system to drive by introducing a catalytic site for the reaction to the system of interest or by choosing a system that already has a suitable catalytic site. After finding a promising combination, we can tune parameters such as the reaction conditions and structures of a substrate (fuel) and a catalyst to achieve the desired nonequilibrium behaviors. Because of its generality, our repurposing approach may offer solutions to a number of problems in constructing chemically driven out-of-equilibrium systems: it not only overcomes the compatibility problem of multiple steps in reaction cycles but also can be a potential solution to the problem of background fuel decomposition because this decomposition via a noncatalyzed pathway is much slower than a fuel consumption by a catalytic cycle that harvests energy. Moreover, this approach may aid in solving the waste accumulation problem, which deteriorates systems' behavior: there is little product inhibition in practical catalytic reactions, which means that waste species will not be harmful to the system if we utilize such a catalytic reaction. Our repurposing approach will bridge the gap between systems chemistry and the field of catalysis, thereby substantially broadening the scope of out-of-equilibrium systems chemistry and helping synthetic systems develop toward the sophistication of biology.

ASSOCIATED CONTENT

Data Availability Statement

The data sets generated during this study and Python codes for the kinetic modeling are available at (https://github.com/hermanslab/AldehydeCatalysis).

Supporting Information

The Supporting Information is available free of charge at https://pubs.acs.org/doi/10.1021/jacs.4c05871.

Materials, methods, synthesis, characterization, additional data, and kinetic modeling (PDF)

Fuel addition experiment with aldehyde **1**, pH = 7.00 (MP4)

Fuel addition experiment with aldehyde **1**, pH = 7.90 (MP4)

Fuel addition experiment without aldehyde **1**, pH = 7.00 (MP4)

Fuel addition experiment without aldehyde **1**, pH = 7.90 (MP4)

AUTHOR INFORMATION

Corresponding Authors

Shuntaro Amano − *University of Strasbourg, CNRS, Strasbourg 67083, France;* orcid.org/0000-0001-6017-6823; Email: samano@unistra.fr

Thomas M. Hermans − *IMDEA Nanociencia, Madrid 28049, Spain;* orcid.org/0000-0003-1121-1754; Email: thomas.hermans@IMDEA.org

Complete contact information is available at: https://pubs.acs.org/10.1021/jacs.4c05871

Notes

The authors declare no competing financial interest.

https://doi.org/10.1021/jacs.4c05871
J. Am. Chem. Soc. 2024, 146, 23289−23296

■ ACKNOWLEDGMENTS

We thank Dr Jorge S. Valera, Dr Marten L. Ploeger, Dr Alex Blokhuis (IMDEA Nanociencia), Dr Emanuele Penocchio (Northwestern University), and Dr Giulio Ragazzon (University of Strasbourg) for insightful discussion and suggestions. We acknowledge support from the European Research Council [ERC Starting Grant 757910 (T.M.H.)].

■ REFERENCES

(1) Amos, L. A. Molecular Motors: Not Quite like Clockwork. *Cell. Mol. Life Sci.* **2008**, *65* (4), 509−515.
(2) Vale, R. D.; Milligan, R. A. The Way Things Move: Looking Under the Hood of Molecular Motor Proteins. *Science* **2000**, *288* (5463), 88−95.
(3) Novák, B.; Tyson, J. J. Design Principles of Biochemical Oscillators. *Nat. Rev. Mol. Cell Biol.* **2008**, *9* (12), 981−991.
(4) Porter, S. L.; Wadhams, G. H.; Armitage, J. P. Signal Processing in Complex Chemotaxis Pathways. *Nat. Rev. Microbiol.* **2011**, *9* (3), 153−165.
(5) Kay, E. R.; Leigh, D. A.; Zerbetto, F. Synthetic Molecular Motors and Mechanical Machines. *Angew. Chem., Int. Ed.* **2007**, *46* (1−2), 72−191.
(6) Corra, S.; Curcio, M.; Credi, A. Photoactivated Artificial Molecular Motors. *JACS Au* **2023**, *3* (5), 1301−1313.
(7) Lancia, F.; Ryabchun, A.; Katsonis, N. Life-like Motion Driven by Artificial Molecular Machines. *Nat. Rev. Chem* **2019**, *3* (9), 536−551.
(8) Das, K.; Gabrielli, L.; Prins, L. J. Chemically Fueled Self-Assembly in Biology and Chemistry. *Angew. Chem., Int. Ed.* **2021**, *60* (37), 20120−20143.
(9) van Rossum, S. A. P.; Tena-Solsona, M.; van Esch, J. H.; Eelkema, R.; Boekhoven, J. Dissipative Out-of-Equilibrium Assembly of Man-Made Supramolecular Materials. *Chem. Soc. Rev.* **2017**, *46* (18), 5519−5535.
(10) Merindol, R.; Walther, A. Materials Learning from Life: Concepts for Active, Adaptive and Autonomous Molecular Systems. *Chem. Soc. Rev.* **2017**, *46* (18), 5588−5619.
(11) van Roekel, H. W. H.; Rosier, B. J. H. M.; Meijer, L. H. H.; Hilbers, P. A. J.; Markvoort, A. J.; Huck, W. T. S.; de Greef, T. F. A. Programmable Chemical Reaction Networks: Emulating Regulatory Functions in Living Cells Using a Bottom-up Approach. *Chem. Soc. Rev.* **2015**, *44* (21), 7465−7483.
(12) Epstein, I. R.; Xu, B. Reaction−Diffusion Processes at the Nano- and Microscales. *Nat. Nanotechnol.* **2016**, *11* (4), 312−319.
(13) Ludlow, R. F.; Otto, S. Systems chemistry. *Chem. Soc. Rev.* **2008**, *37* (1), 101−108.
(14) von Kiedrowski, G.; Otto, S.; Herdewijn, P. Welcome Home, Systems Chemists. *J. Syst. Chem.* **2010**, *1* (1), 1.
(15) Ashkenasy, G.; Hermans, T. M.; Otto, S.; Taylor, A. F. Systems chemistry. *Chem. Soc. Rev.* **2017**, *46* (9), 2543−2554.
(16) Astumian, R. D. Design Principles for Brownian Molecular Machines: How to Swim in Molasses and Walk in a Hurricane. *Phys. Chem. Chem. Phys.* **2007**, *9* (37), 5067.
(17) Pieters, B. J. G. E.; van Eldijk, M. B.; Nolte, R. J. M.; Mecinović, J. Natural Supramolecular Protein Assemblies. *Chem. Soc. Rev.* **2016**, *45* (1), 24−39.
(18) Valiron, O.; Caudron, N.; Job, D. Microtubule Dynamics. *Cell. Mol. Life Sci.* **2001**, *58* (14), 2069−2084.
(19) Singh, N.; Formon, G. J. M.; De Piccoli, S.; Hermans, T. M. Devising Synthetic Reaction Cycles for Dissipative Nonequilibrium Self-Assembly. *Adv. Mater.* **2020**, *32* (20), 1906834.
(20) Biagini, C.; Di Stefano, S. Abiotic Chemical Fuels for the Operation of Molecular Machines. *Angew. Chem., Int. Ed.* **2020**, *59* (22), 8344−8354.
(21) Borsley, S.; Leigh, D. A.; Roberts, B. M. W. Chemical Fuels for Molecular Machinery. *Nat. Chem.* **2022**, *14* (7), 728−738.
(22) Rieß, B.; Grötsch, R. K.; Boekhoven, J. The Design of Dissipative Molecular Assemblies Driven by Chemical Reaction Cycles. *Chem.* **2020**, *6* (3), 552−578.
(23) Amano, S.; Borsley, S.; Leigh, D. A.; Sun, Z. Chemical Engines: Driving Systems Away from Equilibrium through Catalyst Reaction Cycles. *Nat. Nanotechnol.* **2021**, *16* (10), 1057−1067.
(24) Aprahamian, I.; Goldup, S. M. Non-Equilibrium Steady States in Catalysis, Molecular Motors, and Supramolecular Materials: Why Networks and Language Matter. *J. Am. Chem. Soc.* **2023**, *145* (26), 14169−14183.
(25) Wood, C. S.; Browne, C.; Wood, D. M.; Nitschke, J. R. Fuel-Controlled Reassembly of Metal−Organic Architectures. *ACS Cent. Sci.* **2015**, *1* (9), 504−509.
(26) Borsley, S.; Kreidt, E.; Leigh, D. A.; Roberts, B. M. W. Autonomous Fuelled Directional Rotation about a Covalent Single Bond. *Nature* **2022**, *604* (7904), 80−85.
(27) Wilson, M. R.; Solà, J.; Carlone, A.; Goldup, S. M.; Lebrasseur, N.; Leigh, D. A. An Autonomous Chemically Fuelled Small-Molecule Motor. *Nature* **2016**, *534* (7606), 235−240.
(28) Amano, S.; Fielden, S. D. P.; Leigh, D. A. A Catalysis-Driven Artificial Molecular Pump. *Nature* **2021**, *594* (7864), 529−534.
(29) Colomer, I.; Morrow, S. M.; Fletcher, S. P. A Transient Self-Assembling Self-Replicator. *Nat. Commun.* **2018**, *9* (1), 2239.
(30) van der Helm, M. P.; Wang, C.; Fan, B.; Macchione, M.; Mendes, E.; Eelkema, R. Organocatalytic Control over a Fuel-Driven Transient-Esterification Network. *Angew. Chem., Int. Ed.* **2020**, *59* (46), 20604−20611.
(31) Englert, A.; Vogel, J. F.; Bergner, T.; Loske, J.; von Delius, M. A Ribonucleotide ↔ Phosphoramidate Reaction Network Optimized by Computer-Aided Design. *J. Am. Chem. Soc.* **2022**, *144* (33), 15266−15274.
(32) Solís Muñana, P.; Ragazzon, G.; Dupont, J.; Ren, C. Z.-J.; Prins, L. J.; Chen, J. L.-Y. Substrate-Induced Self-Assembly of Cooperative Catalysts. *Angew. Chem., Int. Ed.* **2018**, *57* (50), 16469−16474.
(33) Englert, A.; Majer, F.; Schiessl, J. L.; Kuehne, A. J. C.; von Delius, M. Acylphosphates as Versatile Transient Species in Reaction Networks and Optical Catalyst Screenings. *Chem.* **2024**, *10* (3), 910−923.
(34) Bal, S.; Das, K.; Ahmed, S.; Das, D. Chemically Fueled Dissipative Self-Assembly That Exploits Cooperative Catalysis. *Angew. Chem., Int. Ed.* **2019**, *58* (1), 244−247.
(35) Van Der Helm, M. P.; De Beun, T.; Eelkema, R. On the Use of Catalysis to Bias Reaction Pathways in Out-of-Equilibrium Systems. *Chem. Sci.* **2021**, *12* (12), 4484−4493.
(36) Boekhoven, J.; Brizard, A. M.; Kowlgi, K. N. K.; Koper, G. J. M.; Eelkema, R.; van Esch, J. H. Dissipative Self-Assembly of a Molecular Gelator by Using a Chemical Fuel. *Angew. Chem., Int. Ed.* **2010**, *49* (28), 4825−4828.
(37) Boekhoven, J.; Hendriksen, W. E.; Koper, G. J. M.; Eelkema, R.; van Esch, J. H. Transient Assembly of Active Materials Fueled by a Chemical Reaction. *Science* **2015**, *349* (6252), 1075−1079.
(38) Dambenieks, A. K.; Vu, P. H. Q.; Fyles, T. M. Dissipative Assembly of a Membrane Transport System. *Chem. Sci.* **2014**, *5* (9), 3396−3403.
(39) Tena-Solsona, M.; Rieß, B.; Grötsch, R. K.; Löhrer, F. C.; Wanzke, C.; Käsdorf, B.; Bausch, A. R.; Müller-Buschbaum, P.; Lieleg, O.; Boekhoven, J. Non-Equilibrium Dissipative Supramolecular Materials with a Tunable Lifetime. *Nat. Commun.* **2017**, *8* (1), 15895.
(40) Kariyawasam, L. S.; Hartley, C. S. Dissipative Assembly of Aqueous Carboxylic Acid Anhydrides Fueled by Carbodiimides. *J. Am. Chem. Soc.* **2017**, *139* (34), 11949−11955.
(41) Morrow, S. M.; Colomer, I.; Fletcher, S. P. A Chemically Fuelled Self-Replicator. *Nat. Commun.* **2019**, *10* (1), 1011.
(42) Berrocal, J. A.; Biagini, C.; Mandolini, L.; Di Stefano, S. Coupling of the Decarboxylation of 2-Cyano-2-phenylpropanoic Acid to Large-Amplitude Motions: A Convenient Fuel for an Acid−Base-Operated Molecular Switch. *Angew. Chem., Int. Ed.* **2016**, *55* (24), 6997−7001.
(43) Singh, N.; Lainer, B.; Formon, G. J. M.; De Piccoli, S.; Hermans, T. M. Re-Programming Hydrogel Properties Using a Fuel-Driven Reaction Cycle. *J. Am. Chem. Soc.* **2020**, *142* (9), 4083−4087.
(44) Leira-Iglesias, J.; Sorrenti, A.; Sato, A.; Dunne, P. A.; Hermans, T. M. Supramolecular Pathway Selection of Perylenediimides Mediated by Chemical Fuels. *Chem. Commun.* **2016**, *52* (58), 9009−9012.

https://doi.org/10.1021/jacs.4c05871
J. Am. Chem. Soc. 2024, 146, 23289−23296

(45) Jain, A.; Dhiman, S.; Dhayani, A.; Vemula, P. K.; George, S. J. Chemical Fuel-Driven Living and Transient Supramolecular Polymerization. *Nat. Commun.* **2019**, *10* (1), 450.
(46) Dhiman, S.; Jain, A.; George, S. J. Transient Helicity: Fuel-Driven Temporal Control over Conformational Switching in a Supramolecular Polymer. *Angew. Chem., Int. Ed.* **2017**, *56* (5), 1329−1333.
(47) Sorrenti, A.; Leira-Iglesias, J.; Sato, A.; Hermans, T. M. Non-Equilibrium Steady States in Supramolecular Polymerization. *Nat. Commun.* **2017**, *8* (1), 15899.
(48) della Sala, F.; Maiti, S.; Bonanni, A.; Scrimin, P.; Prins, L. J. Fuel-Selective Transient Activation of Nanosystems for Signal Generation. *Angew. Chem., Int. Ed.* **2018**, *57* (6), 1611−1615.
(49) Heuser, T.; Weyandt, E.; Walther, A. Biocatalytic Feedback-Driven Temporal Programming of Self-Regulating Peptide Hydrogels. *Angew. Chem., Int. Ed.* **2015**, *54* (45), 13258−13262.
(50) Hirst, A. R.; Roy, S.; Arora, M.; Das, A. K.; Hodson, N.; Murray, P.; Marshall, S.; Javid, N.; Sefcik, J.; Boekhoven, J.; Van Esch, J. H.; Santabarbara, S.; Hunt, N. T.; Ulijn, R. V. Biocatalytic Induction of Supramolecular Order. *Nat. Chem.* **2010**, *2* (12), 1089−1094.
(51) Chen, Q.; Lv, Y.; Zhang, D.; Zhang, G.; Liu, C.; Zhu, D. Cysteine and pH-Responsive Hydrogel Based on a Saccharide Derivative with an Aldehyde Group. *Langmuir* **2010**, *26* (5), 3165−3168.
(52) Hay, R. W.; Main, L. Catalysis by aromatic aldehydes and carbon dioxide of the hydrolysis of the p-nitrophenyl esters of L-leucine, glycine, and L-*β*-phenylalanine. *Aust. J. Chem.* **1968**, *21*, 155−169.
(53) Pascal, R. Catalysis through Induced Intramolecularity: What Can Be Learned by Mimicking Enzymes with Carbonyl Compounds That Covalently Bind Substrates? *Eur. J. Org Chem.* **2003**, *2003* (10), 1813−1824.
(54) Yuan, Z.; Liao, J.; Jiang, H.; Cao, P.; Li, Y. Aldehyde Catalysis − from Simple Aldehydes to Artificial Enzymes. *RSC Adv.* **2020**, *10* (58), 35433−35448.
(55) *Asymmetric Organocatalysis: New Strategies, Catalysts, and Opportunities*; Albrecht, Ł., Albrecht, A., Dell'Amico, L., Eds.; WILEY-VCH GmbH, 2022.
(56) Parschau, M. *Organometallics and Catalysis: An Introduction*; Oxford University Press, 2014.
(57) Singh, N.; Lopez-Acosta, A.; Formon, G. J. M.; Hermans, T. M. Chemically Fueled Self-Sorted Hydrogels. *J. Am. Chem. Soc.* **2022**, *144* (1), 410−415.
(58) De Greef, T. F. A.; Smulders, M. M. J.; Wolffs, M.; Schenning, A. P. H. J.; Sijbesma, R. P.; Meijer, E. W. Supramolecular Polymerization. *Chem. Rev.* **2009**, *109* (11), 5687−5754.
(59) Sharko, A.; Livitz, D.; De Piccoli, S.; Bishop, K. J. M.; Hermans, T. M. Insights into Chemically Fueled Supramolecular Polymers. *Chem. Rev.* **2022**, *122* (13), 11759−11777.
(60) Godoy-Alcántar, C.; Yatsimirsky, A. K.; Lehn, J.-M. Structure-stability Correlations for Imine Formation in Aqueous Solution. *J. Phys. Org. Chem.* **2005**, *18* (10), 979−985.
(61) Cordes, E. H.; Jencks, W. P. The Mechanism of Hydrolysis of Schiff Bases Derived from Aliphatic Amines. *J. Am. Chem. Soc.* **1963**, *85* (18), 2843−2848.
(62) *Heterogeneous Catalysts: Advanced Design, Characterization and Applications*; Teoh, W. Y., Urakawa, A., Ng, Y. H., Eds.; WILEY-VCH GmbH, 2021.

https://doi.org/10.1021/jacs.4c05871
J. Am. Chem. Soc. 2024, 146, 23289−23296